RELATION OF THE MAGNETIC PROPERTIES OF CONTROL-ROLLED PIPE STEEL TO ITS STRUCTURAL ANISOTROPY, INTERNAL STRESSES AND DAMAGE

E. S. GORKUNOV, S. Yu. MITROPOLSKAYA, S. M. ZADVORKIN,
L. S. SHERSHNEVA, D. I. VICHUZHANIN, E. A. TUYEVA
INSTITUTE OF ENGINEERING SCIENCE, RAS (Ural Branch), Ekaterinburg, Russia

Main pipelines are characterized by a highly indeterminate stress-strain state of pipes and complex conditions of thermomechanical loading, the principal loads being internal pressures and stresses in metal caused by differences in pipeline construction and use conditions resulting from soil mobility, non-design loads during floods etc. [1]. Therefore it seems urgent to develop reliable methods of estimating stress loading and damage of metal, which would offer advice on optimising pipeline service conditions and conclusions on the strength and safety of a system in the attempt to increase its durability [2].

The applicability of magnetic methods to the estimation of working stresses in pipelines is discussed in a number of studies made on hot-rolled pipe steels like St2, St4, 17G1S [3, 4]. However, much of pipeline steel is currently produced by controlled rolling, when higher strength and cold-resistance are attained due to lower temperature and higher extent of reduction in the final stages of rolling. Recrystallization and the growth of austenite grain therewith slow down, particularly, in the presence of dispersed precipitations of carbonitrides [1]. The fall of the rolling end temperature to the (γ+α)-region leads to the formation of ferrite grains with high dislocation density and a pronounced strain texture [5]; this affects magnetic properties considerably and one must taken it into account when developing magnetic techniques for estimating the state of pipelines.

This paper seeks approaches to estimating internal stresses, as well as working stresses and damage, of control-rolled pipe steel by magnetic characteristics measured under uniaxial stress and torsion.

Material and Procedure

Test specimens were cut out of a longitudinally welded (LW) pipe and a spirally welded (SW) one made of control-rolled metal of the strength class X70 (API classification). The chemical composition of the steels examined is given in Table 1. Both variants are classified as low-carbon low-alloy steels, one (X70LW) being mono-microalloyed by niobium, and the other (X70SW) containing molybdenum and vanadium. The specimens were cut out across and along the sheet rolling direction, and in the instance of an SW pipe also along and across the pipe axis (i. e., at angles of about 40° and 130° to the direction of rolling). To avoid the influence of machining on the value of internal stresses in the specimens, the surface layer was removed by electropolishing.

Table 1. The chemical composition of the steels

	Fraction, weight %										
	C	Mn	Si	S	P	Cr	Ni	Mo	V	Al	Nb
X70LW	0.098	1.620	0.434	0.0008	0.011	0.024	0.046	0.009	0.002	0.033	0.050
X70SW	0.060	1.620	0.180	0.003	0.015	0.040	0.020	0.24	0.068	0.040	0.050

The effect of internal stresses on the magnetic characteristics of steels was studied on specimens cut out across the axes of LW and SW pipes. The level of internal stresses in these specimens was varied by isothermal annealing sequentially at 200, 300, 400, 500 and 600°C, with holding at each temperature within 2 hours and subsequent cooling with the oven. Thus, the total

duration of annealing was 12 hours. After each step of annealing, the specimens were electropolished in order to remove the oxidized layer, residual stresses in them were evaluated by X-ray diffraction analysis and magnetic characteristics were measured. The specimens were also examined in the initial condition, without annealing. The lattice microdistortions were calculated by the moment method [6], by the (211) X-ray reflection of the α-phase. Note that crystal lattice distortions are detected by X-ray diffraction analysis. To calculate internal stresses by these data, one needs to know the behaviour of metal microvolume deformation and the laws relating strains to stresses on the microscopic level. Therefore in what follows, when direct experimental data are adduced, it is crystal lattice distortions that are discussed.

The magnetic characteristics of the specimens were measured in a closed magnetic permeameter-type circuit both after sequential annealing intended for varying the level of residual stresses and under applied loading. In both cases the magnetic field was applied along the long specimen axes, i. e., the magnetic field intensity vector was parallel to the applied load in tension and the torsional axis in torsion. The coercive force H_C and residual induction B_r, maximum magnetic permeability μ_{max} and the field of maximum magnetic permeability $H(\mu_{max})$ were determined by major hysteresis loops. The magnetic parameters after each annealing step were also measured by a magnetic structuroscope equipped with an attached electromagnetic sensor (AES).

Tension and torsion tests were made at room temperature up to specimen fracture. Magnetic measurements were made up to necking (in tension) and up to specimen fracture (in torsion).

The microstructure was studied on an optical microscope and a raster electronic microscope.

The Effect of Structural Anisotropy on Magnetic and Mechanical Properties of Control-Rolled Steels

The structure of the specimen cut out of an LW pipe consists of deformed and polygonal ferrite and low-temperature austenite decomposition products (bainite regions in the form of extensive bands and martensite islets).

The structure of the specimen cut out of an SW pipe is ferrite of different morphology with inclusions of bainite-martensite mixture in the form of discontinuous lines. The direction of rolling is revealed by the orientation of these lines and by the stretching of ferrite grains. The microstructure is characterized by low density. On the metallographic section made through the sheet thickness across the direction of rolling the structure becomes isotropic with much dispersed ferrite grains uniform in size. The microstructure of the surface layers, which cooled down faster, differs from the structure of internal regions in that highly dispersed products of low-temperature decay are intensively generated, including those of acicular morphology.

The mechanical properties of specimens cut out in different directions are given in Table 2. As is obvious, in the instance of an LW pipe the strength characteristics of the metal lack anisotropy. This may be due to the removal of the rolling-induced anisotropy during metal deformation in pipe shaping. For the metal of an SW pipe, the highest values of ultimate stress σ_u and conventional yield stress $\sigma_{0.2}$ were obtained on the specimens cut out across the direction of rolling. This relation between the strength properties of rolled products and the direction of sampling is governed by the formation of a crystallographic texture with the orientation {112}(110) [7].

The data found in Table 2 suggest that B_r and μ_{max} are sensitive to the structural anisotropy of steel after controlled rolling both in the LW pipe and in the SW one. For instance, in magnetization along the direction of rolling, i. e. along the long axis of the main structural elements, μ_{max} is about 40 % higher than in magnetization across the direction of rolling. In the measurements taken in the other two directions of cutting the SW pipe specimens, μ_{max} takes intermediate values. The coercive force in the LS pipe is maximal when measurements are made across the direction of rolling, since the density of the grain boundaries is maximal in this direction, and hence, obstacles and possible pinning sites are most numerous on the way of domain wall motion in magnetization reversal. At the same time, the anisotropy of the coercive force value in the SW pipe is poorly pronounced due to the peculiarities of steel sheet shaping in making pipes of this type (the direction of rolling makes an angle of about 40° with the longitudinal pipe axis).

Table 2. Mechanical and magnetic properties of specimens made of steels of strength group X70

Direction of specimen cutting	σ_u, MPa	$\sigma_{0.2}$, MPa	δ, %	ψ, %	H_C, A/cm	B_r, T	μ_{max}
LW pipe							
Along the pipe axis	600	535	9.0	71	6.17	1.17	835
Across the pipe axis	600	532	10.5	70	7.40	0.70	450
Across the pipe axis, annealing 500 °C	585	490	12.0	68	4.31	1.23	1116
SW pipe							
Along the direction of rolling	610	545	10.7	70	5.80	1.23	1110
Across the direction of rolling	665	595	11.3	66	5.92	0.99	770
Along the pipe axis	600	545	6.8	69	5.43	1.08	855
Across the pipe axis	570	485	29.0	84	4.80	1.06	925
Across the pipe axis, annealing 500 °C	570	510	20.0	80	4.5	1.164	1066

Note: δ is specific elongation, ψ is specific necking.

The highest residual magnetic induction (B_r = 1.23 T) was recorded when the direction of magnetization coincides with the direction of ferrite grains and line precipitates, i. e., the demagnetising factor of crystallites is minimal. In magnetization across the axis of rolling, B_r in steel X70LW is much lower, than in steel X70SW in the same direction (0.70 and 0.99 T, respectively).

Also, an experiment was made to study the effect of annealing at 500°C within 2 hours on the mechanical and magnetic characteristics of steels of strength group X70. This annealing imitated thermal treatment of pipes aimed at relieving internal stresses in the weld and in the metal of the near-weld zone. The level of the strength properties of the steels is seen to decrease slightly when the magnetic characteristics change notably. Particularly, H_C decrease reached 40%.

Thus, the structure of control-rolled steel is characterized by non-uniform grain dimensions, streakiness, a mixture of structural components of different types and crystallographic texture in ferrite. In the absence of external loads, such magnetic characteristics of the SW pipe metal as B_r and μ_{max} depend on the direction of magnetization relative to the direction of rolling and correlate with the strength properties. In the direction of rolling, when μ_{max} assumes the highest values, the strength characteristics of the metal are minimal. In the cross direction the lowest values of μ_{max} and the maximum level of strength properties. For the LW pipe, dependences of the kind are not observed, as there is no anisotropy of strength properties.

The Effect of Crystal Lattice Microdistortions on Magnetic Characteristics

Figure 1*a* shows the magnitude of crystal lattice microdistortions as dependent on the temperature of annealing (T_{an}) for specimens cut out across LW and SW pipes. The initial level of crystal lattice microdistortions for the SW specimen is 20% higher than that for the LW one. It is first of all due to differences in the production process (shaping) for LW and SW pipes. Besides, allowance should be made for the fact that the pipes of these kinds are made of metal sheets differing in their chemical compositions. Rolling parameter spread is also inevitable in the course of

metal working (reduction degree, rolling end temperature and rate cooling). As the temperature of isothermal holding rises from 200°C to 600°C, especially at temperatures over 400°C, a significant decrease in crystal lattice distortions is observed for both steels. The coercive force also decreases monotonically as T_{an} rises. As to residual induction and maximum magnetic permeability, they, on the contrary, rise with the temperature of annealing. Consequently, in both steels the coercive force grows with the increase of crystal lattice microdistortions, whereas residual induction and maximum magnetic permeability decrease (Fig.1*b*). The dependences for the SW pipe are described by a linear function, and for the LW one by a nonlinear one. The uniqueness of these dependences allows H_C, B_r and μ_{max} to be used as test parameters in the estimation of internal stresses in control-rolled pipe steels.

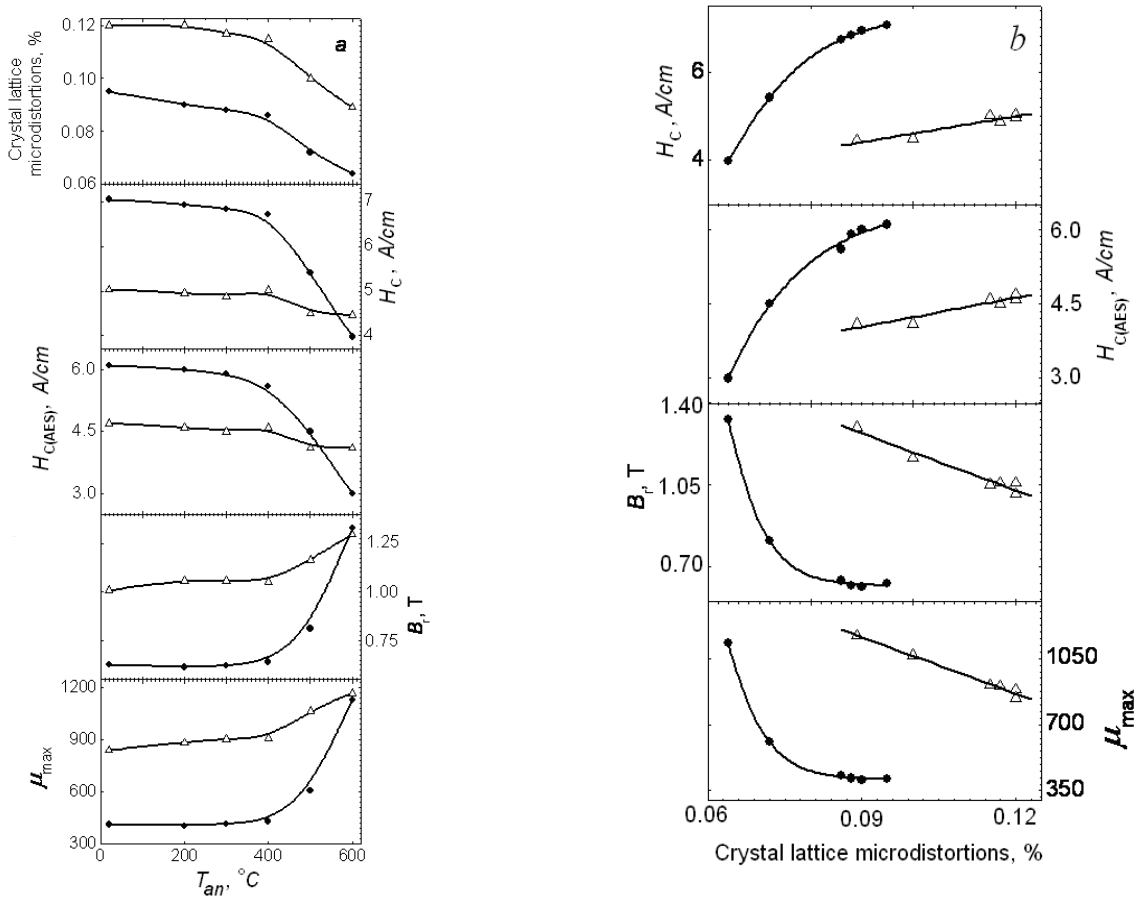

Fig. 1. Crystal lattice microdistortions, coercive force, residual induction and maximum magnetic permeability, all measured in a closed magnetic circuit, and coercive force measured by an attached electromagnetic sensor as functions of annealing temperature for specimens cut out of an LW pipe (•) and an SW pipe (Δ) (*a*); magnetic characteristics as functions of crystal lattice microdistortions for the steels studied (*b*).

It is obvious from Fig. 1 that the values of $H_{C(AES)}$ (the coercive force determined with the use of an attached electromagnetic sensor) are approximately 20% lower than those when measured in a closed magnetic circuit. However, the lattice microdistortion dependences of H_C and $H_{C(AES)}$ are qualitatively similar. Thus, the coercive force determined by attached magnetic devices can also serve as a parameter in estimating internal stresses in control-rolled steels.

Determination of the Damage Parameter

To characterise defects arising during deformation, mechanical scientists use a parameter termed “damage”. The value of damage estimates a current state of a material being studied. The

parameter ω can enable one to estimate the durability of machine parts and structural members working in various loading conditions. The predictability of the fracture of die tooling under cyclic loading is discussed In [8–9] it is demonstrated how the magnitude of damage can be used to predict the fracture of die tooling under cyclic loading.

According to the fracture theory [10], it is assumed that damage is zero before the deformation process starts, and that it becomes $\omega = 1$ by the instant of specimen fracture. It was found in [11] that the damage values $\omega = 0.2$ to 0.3 correspond to the formation of submicrodefects in a metal (submicrocracks and submicropores smaller than 0.1…0.5 μm), which are in the state of elastic equilibrium with the metal matrix, and to the elastic detachment of the metal matrix from inclusions. The values of damage $\omega = 0.6$ to 0.7 correspond to the formation of micropores and microcracks within the size of the metal structure elements (grains, phase components, inclusions).

Damage in torsion (to fracture) and uniaxial tension (to necking) was calculated by the accumulated amount of strain with the application of a linear model of damage accumulation authored by V. L. Kolmogorov [12]. The results obtained are presented in Fig. 2.

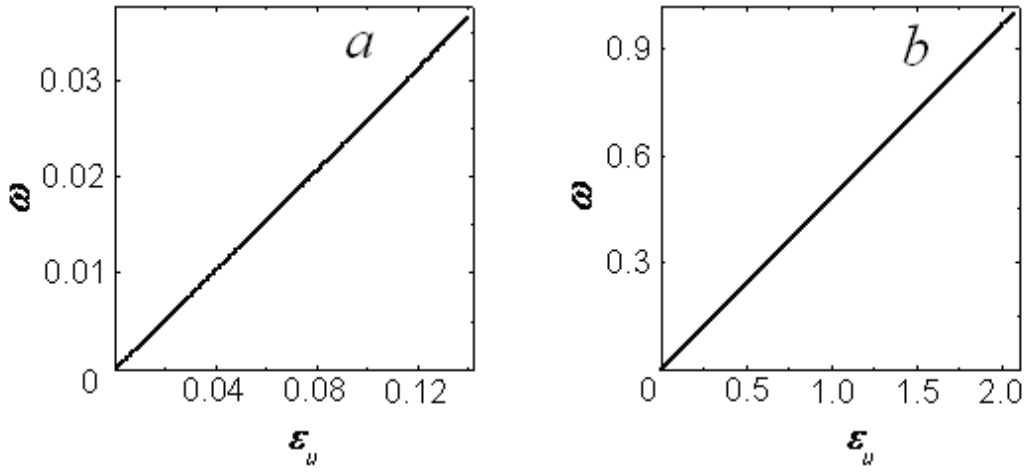

Fig. 2. Damage as a function of uniaxial tensile deformation to necking (*a*) and torsional deformation to fracture (*b*).

The fractograph of the specimen fracture surface after uniaxial tension testing is given in Fig. 3. The fracture surface is seen to be characteristic of ductile fracture. The fracture surfaces of the other specimens are of a similar nature.

Micropores and other discontinuities, which are responsible for material damage, behave as nonmagnetic inclusions causing lower saturation magnetization J_{max} and higher H_C. This is demonstrated by the dependences shown in Fig. 4, where the change in the coercive force H_C and saturation magnetization under tension (*a*) and torsion (*b*) of specimens cut out across the pope axis is shown as a function of the damage parameter.

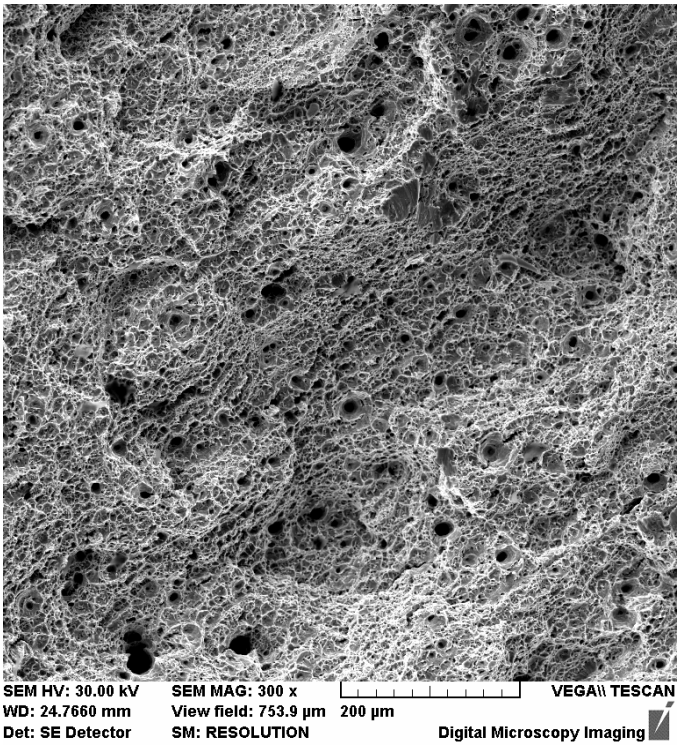

Fig. 3. The fracture surface of a specimen cut out across the pipe axis after tensile testing (steel X70), × 300.

The curves attest that the coercive force grows monotonically with torsional damage and that the saturation magnetization decreases. This is a manifestation of accumulation of crystal lattice defects, micropores, microcracks etc. Under tension, due to the positive magnetoelastic effect [13], H_C behaves ambiguously, namely, the coercive force decreases prior to the values of ω equal to 4×10^{-4}, and the further accumulation of tensile damage leads to a notable growth of H_C. The saturation magnetization decreases monotonically, as in torsion.

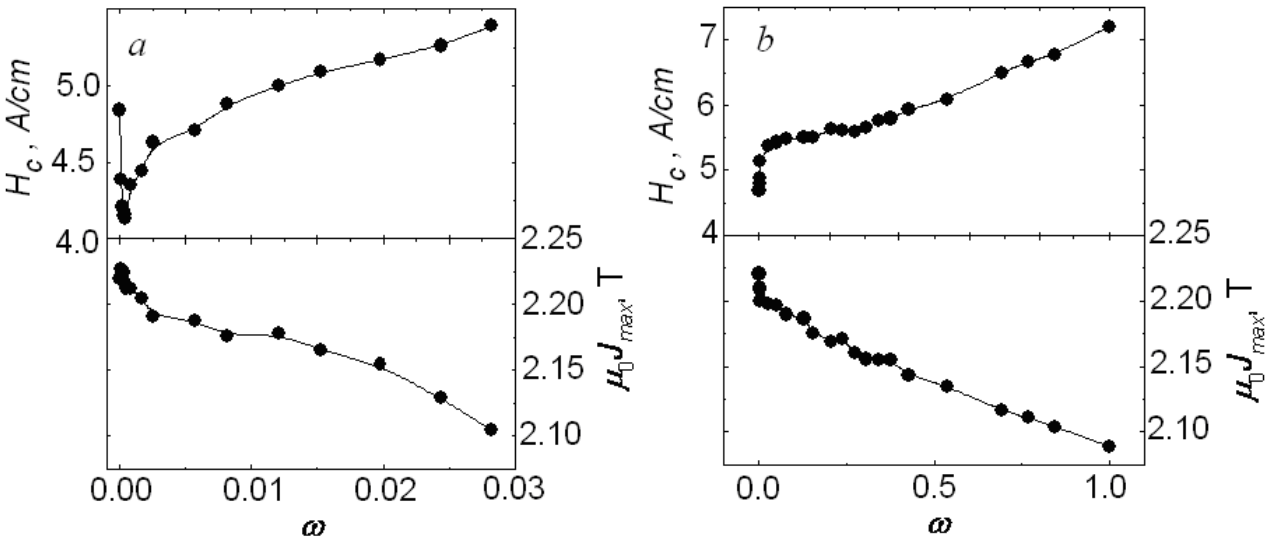

Fig. 4. The coercive force H_C and saturation magnetization J_{max} for steel X70 as a function of the damage parameter in tension (*a*) and torsion (*b*).

Figure 5 shows the varying magnetic characteristics of specimens made of steel X70, which were cut out of an LW pipe (*a*) and an SW one (*b*) in different directions under applied uniaxial tensile stresses. The behaviour of the dependences is similar for both pipes. In the initial stages of stressing, the coercive force decreases reaching its minimum at stresses of about 200 to 250 MPa. As mentioned above, this results from the magnetoelastic effect. Simultaneously with the decrease in the coercive force, there is an increase in residual induction and maximum magnetic permeability. On the further increase of stressing, the dependences behave oppositely, i. e., the coercive force grows, whereas the residual induction and maximum magnetic permeability decrease. Note that the anisotropy of magnetic properties in the metal of the LW pipe persists in the entire range of applied loads, whereas in the metal of the SW pipe this anisotropy is noticeable only in the initial stage of stressing.

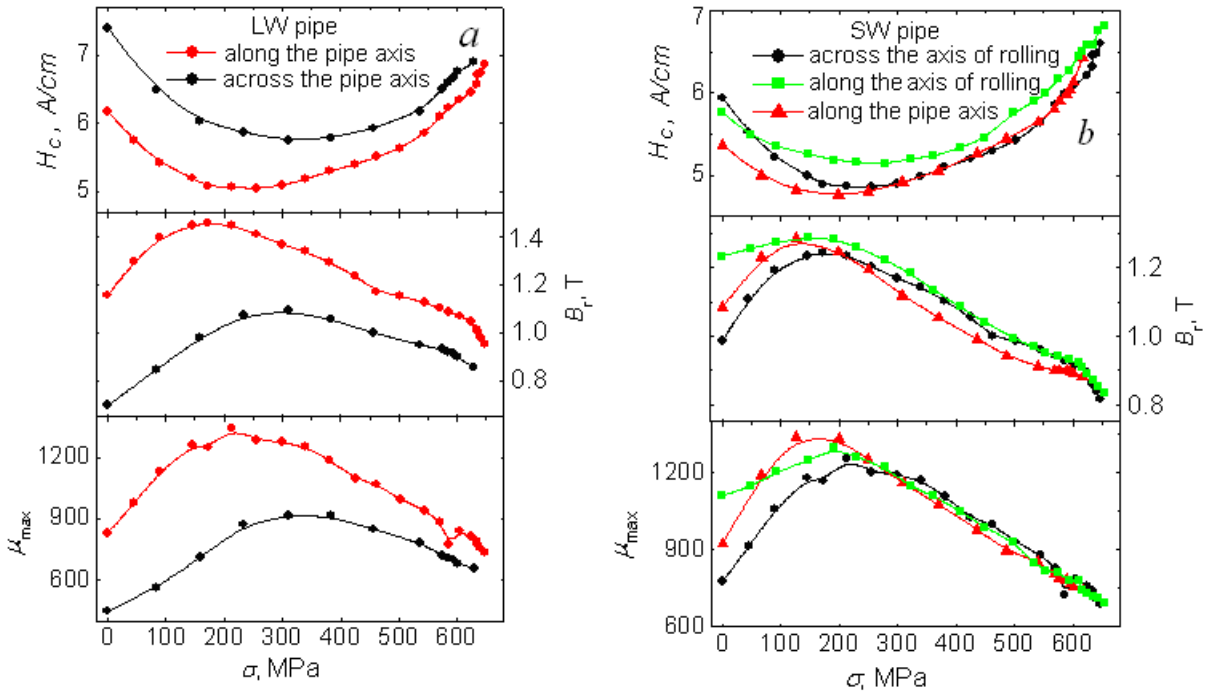

Fig. 5. The magnetic characteristics of steel X70 as functions of applied tensile stresses.

In the instance of shearing stresses τ, as distinct from tension, H_C grows monotonically, whereas B_r and μ_{max} decrease (Fig. 6). Note that in the vicinity of the conventional yield stress ($\tau_{0.3} \cong 315$ MPa) on the dependence $B_r(\tau)$ there is a local minimum of residual induction. However, B_r varies within the range of measuring accuracy. At stresses $\tau \geq 650$ MPa the magnetic characteristics of the steels vary heavily. This is attributed to a considerable growth of material damage on this stage of deformation. On the dependences $H_C(\sigma)$, $B_r(\sigma)$ and $\mu_{max}(\sigma)$ shown in Fig. 5 this heavy variation of magnetic characteristics is not observed, since, as mentioned above, the magnetic characteristics under tension were measured only to necking, i. e., at comparatively low values of ω, see Fig. 1.

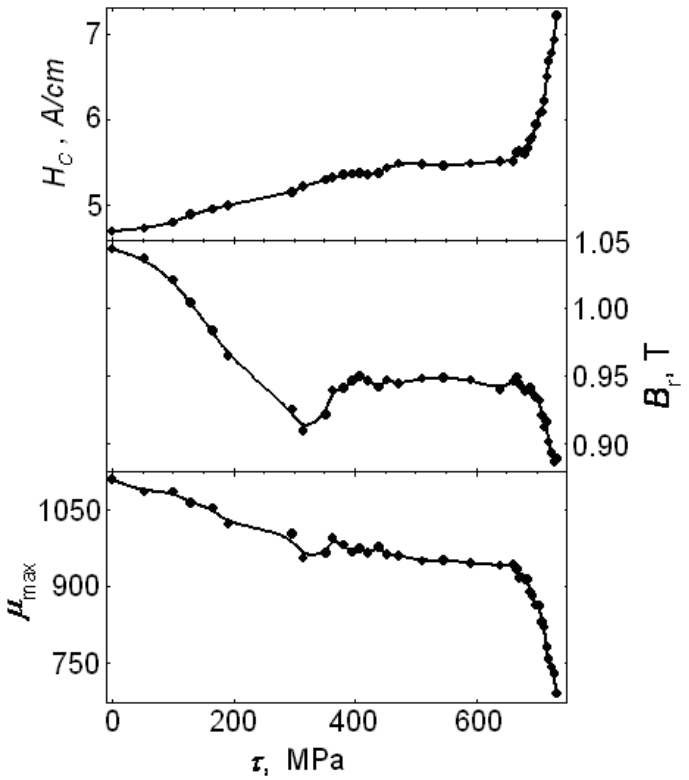

Fig. 6. The magnetic characteristics of steel X70 as functions of applied shearing stresses.

The study was partially supported by the RFBR (grant no 09-08-01091-a), the RAS Presidium (project "Fundamental problems of interaction mechanics in engineering and natural systems") and the RAS Department of Power Engineering, Mechanical Engineering, Mechanics and Control Processes (project "Tribological and strength properties of structured materials and surface layers").

REFERENCES

1. Anuchkin M. P., Miroshnichenko B. I., Goritsky V. N. Pipes for mains. M.: Nedra, 1986. 231 p.
2. Frolov K. V., Makhutov N. A., Khurshudov G. Kh., Gadenin M. M. Strength, durability and safety of engineering systems // Strength problems. 2002, no 5, pp. 8–18.
3. Teplinsky Yu. A., Aginey R. V., Kuzbozhev A. S., Andronov I. N. A Investigation into the peculiarities of changes in magnetic parameters of steel 17G1S under uniaxial tensile stressing // Kontrol. Diagnostika. 2004, no 12, pp. 6–8.
4. Aginey R. B., Kuzbozhev A. A. Modelling the state of steel in the evaluation of mechanical stresses by coercive force // Tekhnologiya metallov. 2006, no1, pp. 14–16.
5. Matrosov Yu. I., Litvinenko D. A., Golovanenko S. A. Steel for main pipelines. M.: Metallurgiya. 1989, 288 p.
6. Rusakov A. A. Metal radiography. M.: Atomizdat, 1977, 480 p.
7. Khaisterkamp F., Khulka K, Matrosov Yu. I. Niobium-containing low-alloy steels, SP Intermet Engineering. M.: 1994, 94 p.
8. Lapovok R. E., Smirnov S. V, Shveikin V. P. Modelling of the fracture of die steel caused by erosion cracks under cyclic thermomechanical effect // Kuznechno-shtampovochnoye proizvodstvo, 1997, no 8, pp. 11–14
9. Biba N. V., Stebunov S. A., Smirnov S. V., Vichuzhanin D. I. Prediction of metal fracture in cold die-forging with the application of an adaptive fracture model // Kuznechno-shtampovochnoye proizvodstvo, 2003. no 3, pp. 39 – 44.
10. Kolmogorov V. L. Mechanics of Plastic metal forming. Ekaterinburg,: UGTU – UPI, 2001. 836 p.

11. Bogatov A. A., Mizhiritsky O. I., Smirnov S. V. Metal plasticity margin in metal forming. M.: Metallurgiya, 1984, 144 p.
12. Kolmogorov V. L. Stresses, strains, fracture. M.:Metallurgiya, 1970, 230 p.
13. Vonsovsky S. V., Shur Ya. S. Ferromagnetism. M.-L.: OGIZ, 1948, 816 p.